JVI Journals.ASM.org

Structure of Serotype 1 Reovirus Attachment Protein σ1 in Complex with Junctional Adhesion Molecule A Reveals a Conserved Serotype-Independent Binding Epitope

Eva Stettner,[a*] Melanie H. Dietrich,[a] Kerstin Reiss,[a*] Terence S. Dermody,[b,c,d] Thilo Stehle[a,d]

Interfaculty Institute of Biochemistry, University of Tübingen, Tübingen, Germany[a]; Departments of Pathology, Microbiology, and Immunology[b] and Pediatrics[d] and Elizabeth B. Lamb Center for Pediatric Research,[c] Vanderbilt University School of Medicine, Nashville, Tennessee, USA

Mammalian orthoreoviruses use glycans and junctional adhesion molecule A (JAM-A) as attachment receptors. We determined the structure of serotype 1 reovirus attachment protein σ1 alone and in complex with JAM-A. Comparison with the structure of serotype 3 reovirus σ1 bound to JAM-A reveals that both σ1 proteins engage JAM-A with similar affinities and via conserved binding epitopes. Thus, σ1–JAM-A interactions are unlikely to explain the differences in pathogenesis displayed by these reovirus serotypes.

Engagement of receptors by viruses initiates infection and influences cell and tissue tropism in the host. While structures of viral ligands bound to receptors are known for some viruses, the binding mode is often based on an exemplary serotype, making it difficult to link serotype-specific differences in tropism with differences in receptor recognition. Mammalian orthoreoviruses (reoviruses) are a useful model for such studies, as the serotypes display striking differences in neural tropism yet engage the same protein receptor, the tight-junction component junctional adhesion molecule A (JAM-A) (1, 2). In addition, serotype 1 (T1) reovirus uses the glycan portion of GM2 as a receptor (3), whereas serotype 3 (T3) reovirus engages a range of sialylated glycans (4–7).

The crystal structure of the trimeric reovirus attachment protein σ1 bound to the membrane-distal immunoglobulin-like D1 domain of JAM-A identified a JAM-A-binding site on the lower part of the T3 σ1 head domain (8). As the sequences of the T1 and T3 σ1 proteins are not well conserved (9), we determined the structure of the T1 σ1 head in complex with JAM-A at 3.2 Å resolution to identify possible differences in JAM-A receptor recognition among the reovirus serotypes. We also determined the structure of the unliganded T1 σ1 head at 2.2 Å resolution to determine whether JAM-A induces structural changes in T1 σ1.

To determine the structure of the unliganded T1 σ1 head (amino acids 308 to 470), we crystallized a construct with a His tag and a trimeric version of the coiled-coil domain of the yeast transcription factor GCN4 (general control nonderepressible 4) (3, 10, 11). The tag was removed for surface plasmon resonance (SPR) experiments. After tag removal, eight non-σ1 amino acids remain at the N terminus as a result of the construct design. These amino acids are distant from the JAM-A-binding site. For complex formation with JAM-A D1 (8), we used a different T1 σ1 construct in which amino acids 308 to 470 were cloned into the pET-15b vector, yielding only two additional amino acids at the N terminus. A complex consisting of T1 σ1 and JAM-A D1 was formed from T1 σ1 purified by JAM-A affinity chromatography. Clarified supernatant containing T1 σ1 was loaded onto a GSTrap column (GE Healthcare) containing glutathione *S*-transferase-tagged JAM-A D1 (8). On-column incubation with thrombin released the σ1–JAM-A complex, which was concentrated to 3.6 mg/ml. Crystals were obtained in 0.1 M morpholineethanesulfonic acid (MES; pH 6.9)–17.1% polyethylene glycol 20000 and flash-frozen with 20% methylpentanediol as a cryoprotectant. Data were collected at the PX III beamline of the Swiss Light Source and processed with XDS (12). The structure was solved by molecular replacement with Phaser (13) by using homology-truncated T3 σ1 and JAM-A (3EOY). Refinement was completed with Phenix (14) and Buster (15). Models were built with Coot (16). Data collection and refinement statistics are provided in Table 1. Structural figures were prepared with PyMOL (17).

The T1 σ1 head is a symmetric trimer with intermolecular contacts that are essentially identical to those observed in the T3 σ1 head (9). Each T1 σ1 monomer engages JAM-A D1 (Fig. 1) in a manner similar to that observed in the T3 σ1 head–JAM-A D1 complex (8). In both complexes, JAM-A is bound at the lower edge of the β-barrel forming the σ1 head, with several contacts involving the 3_{10} helix in the D-E loop. JAM-A also forms contacts with residues in the body domain located beneath the head (Fig. 1A). The combined contact areas for the complexes are similar in size, 1,644 Å^2 for T1 (Fig. 1D) and 1,622 Å^2 for T3 (8). However, the hydrogen bonding network encompasses the entire contact area on T1 σ1, whereas hydrogen bonds are restricted to the contact area on the T3 σ1 head, dividing the contact area into two

Received 16 February 2015 **Accepted** 17 March 2015

Accepted manuscript posted online 25 March 2015

Citation Stettner E, Dietrich MH, Reiss K, Dermody TS, Stehle T. 2015. Structure of serotype 1 reovirus attachment protein σ1 in complex with junctional adhesion molecule A reveals a conserved serotype-independent binding epitope. J Virol 89:6136–6140. doi:10.1128/JVI.00433-15.

Editor: S. López

Address correspondence to Thilo Stehle, thilo.stehle@uni-tuebingen.de, or Terence Dermody, terry.dermody@vanderbilt.edu.

* Present address: Eva Stettner, Institute for Biochemistry and Biology, University of Potsdam, Potsdam, Germany; Kerstin Reiss, Institute of Complex Systems (ICS-6), Forschungszentrum Juelich, Juelich, Germany.

doi:10.1128/JVI.00433-15

TABLE 1 Data collection and refinement statistics

Statistic	T1 σ1	T1 σ1–JAM-A complex
Data collection		
Space group	$I2_12_12_1$	$P3_121$
Unit cell dimensions (Å)	a = 112.9, b = 113.0, c = 113.2	a = b = 156.8, c = 96.5
Unit cell angle(s) (°)	α = β = γ = 90	α = β = 90, γ = 120
Resolution range (Å)	50–2.20 (2.26–2.20)[a]	50.00–3.20 (3.28–3.20)
Completeness (%)	98.7 (98.9)	99.1 (99.5)
No. of unique reflections	36,975	22,673
Redundancy (fold)	5.1	4.8 (3.8)
R_{meas} (%)[b]	13.0 (131.8)	8.6 (43.8)
$R_{mrgd\text{-}F}$ (%)[b]		11.1 (50.6)
$I/\sigma I$ ratio	11.7 (1.6)	14.8 (3.3)
Refinement		
Resolution range (Å)	42.32–2.20 (2.26–2.20)	41.00–3.20 (3.28–3.20)
R_{work} (%)	19.1	21.1 (25.9)
R_{free} (%)[c]	22.2	24.3 (30.0)
No. of protein atoms	3,797	6,276
B factor (Å^2)		
Protein	38.0	81.6
σ1		62.8
JAM-A		112.1
No. of molecules		
Water	94	
Cl^-	3	
Mg^{2+}	3	
Acetate	3	
Glycerol	7	
B factor (Å^2)		
Water	48.1	
Cl^-	49.7	
Mg^{2+}	51.0	
Acetate	63.4	
Glycerol	53.7	
RMSD[d]		
Bond lengths (Å)	0.010	0.009
Bond angles (°)	1.100	1.200
Ramachandran plot[e]		
Most favorable regions (%)	97.1	96.0
Additional allowed regions (%)	2.9	4.0
Generously allowed regions (%)	0	0
Disallowed regions (%)	0	0

[a] Values in parentheses refer to the outermost resolution shell.
[b] As defined by Diederichs and Karplus (28).
[c] Free set (29) contains 10% of the data.
[d] RMSD, root mean square deviation.
[e] Calculated with Rampage (26, 30).

parts (Table 2). Contacts formed by residues in the highly conserved 3_{10} helix of T1 σ1 are nearly identical to those in the T3 σ1–JAM-A complex. An additional hydrogen bond exists between T1 residue Gln396 and the main-chain nitrogen atom of Arg59 in JAM-A. This interaction cannot be formed by the equivalent residue of T3 σ1, which is a leucine. Interactions surrounding the 3_{10} helix are also similar in both complexes. The side chain of T1 residue Glu401 is shifted upward and interacts with JAM-A Tyr75 in addition to Asn76 and Lys78. The lower contact area is more polar in T1, where Arg312 and Arg329 contact the JAM-A F-G loop. Arg329 is replaced by an asparagine in T3, which cannot form similar contacts. The different contacts lead to slightly dif-

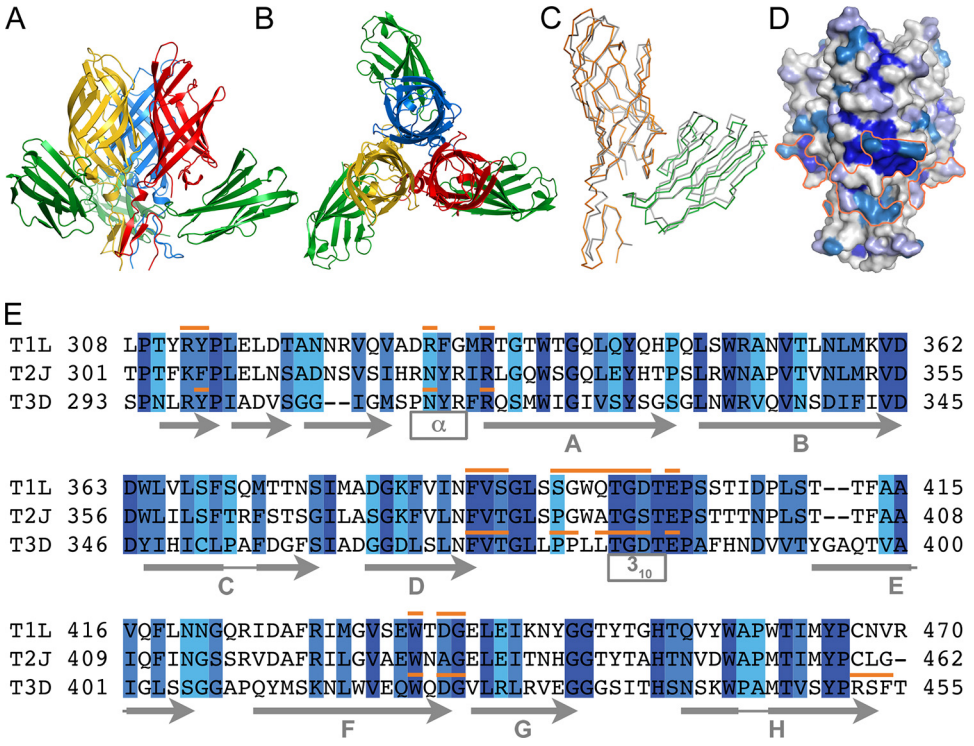

FIG 1 Structure of the T1 σ1–JAM-A complex and conservation of the JAM-A-binding site on σ1. Ribbon tracing showing the complex from the side (A) and the top along the trimer axis (B). The σ1 protein is red, yellow, and blue; JAM-A is green. (C) Cα tracing of the T1 σ1–JAM-A complex. T1 σ1 is orange; JAM-A is green. One subunit of the T3 σ1–JAM-A complex is superposed in gray (PDB code 3EOY). (D) JAM-A contact area on T1 σ1. The σ1 protein is shown in a surface representation. Residues are colored according to conservation among T1 (Lang strain, T1L), serotype 2 (Jones strain, T2J), and T3 (Dearing strain, T3D) from dark blue to light blue. The JAM-A contact area is outlined in orange. (E) Clustal W alignment (25) of the σ1 head domains of strains T1L, T2J, and T3D colored as in panel D. T1 and T3 residues contacting JAM-A within 5 Å are marked in orange.

ferent binding angles of JAM-A D1 in the respective complexes (Fig. 1C). The different angles are unlikely to result from crystal packing, as there are several copies of each complex present in the asymmetric units of the two structures.

TABLE 2 JAM-A-contacting residues in T1 σ1 aligned with T3 σ1[a]

T1 σ1	T3 σ1	Location
Arg312[b]	Arg297	β spiral (body)
Tyr313	Tyr298	
Arg329[b]	Asn312	α helix between head and body
Arg333	*Arg316*	β strand A
Phe387	*Phe370*	D-E loop
Val388[c]	*Val371*[c]	
Ser389	Thr372	
Ser393	Pro376	
Gly394	Pro377	
Trp395	Leu378	
Gln396[b]	Leu379	
Thr397[c]	*Thr380*[c]	3_{10} helix in D-E loop
Gly398[c]	*Gly381*[c]	
Asp399[b]	Asp382[b]	
Glu401[b]	*Glu384*[b]	D-E loop
Trp436	*Trp421*	β strand F
Asp438[b]	Asp423[b]	F-G loop
Gly439	*Gly424*	

[a] Residues in italics are conserved in prototype reovirus strain T1L, T2J, and T3D σ1.
[b] Residue forming a hydrogen bond or salt bridge with JAM-A D1 via side-chain interaction.
[c] Residue forming a hydrogen bond or salt bridge with JAM-A D1 via main-chain interaction.

To determine the affinities of T1 and T3 σ1 for JAM-A, we performed SPR experiments with a Biacore 2000 (GE Healthcare). C-terminal regions of T1 σ1 (56 kDa) or T3 σ1 (53 kDa, amino acids 293 to 455) trimers (18) were immobilized on a CM5 biosensor chip at a density of 25 to 60 resonance units (RU) with 1-ethyl-3-(3-dimethylaminopropyl)carbodiimide hydrochloride–*N*-hydroxysuccinimide coupling chemistry. Deactivated flow cells served as a reference. JAM-A D1D2 (23 kDa, amino acids 27 to 233) (19) was serially diluted 2-fold and injected onto the biosensor surface for 300 s with a dissociation time of 500 s and a flow rate of 50 μl/min. Data were reference subtracted, solvent corrected, and evaluated with BIA evaluation software (GE Healthcare) and OriginPro (OriginLab, Northampton, MA). In each case, three or four independent experiments were performed with two different chips. Both complexes display high nanomolar affinities, with averaged K_d values of 2.0 (± 0.1) × 10^{-7} M for T1 and 5.3 (± 0.5) × 10^{-7} M for T3 (Fig. 2). Because of high on and off rates of JAM-A binding to T1 and T3 σ1, kinetic parameters of the interaction could not be determined. These K_d values are consistent with the comparable contacts in the crystal structures.

The conservation of the JAM-A-binding site on T3 σ1 (8) suggested that the other reovirus serotypes engage JAM-A in a similar manner. The T1 σ1 head–JAM-A D1 structure now provides evidence that this is indeed the case. Our analysis establishes that differences in tropism between T1 and T3 reoviruses are unlikely to be attributable to differential recognition of JAM-A. Instead, we think it possible that recognition of different carbohydrate core-

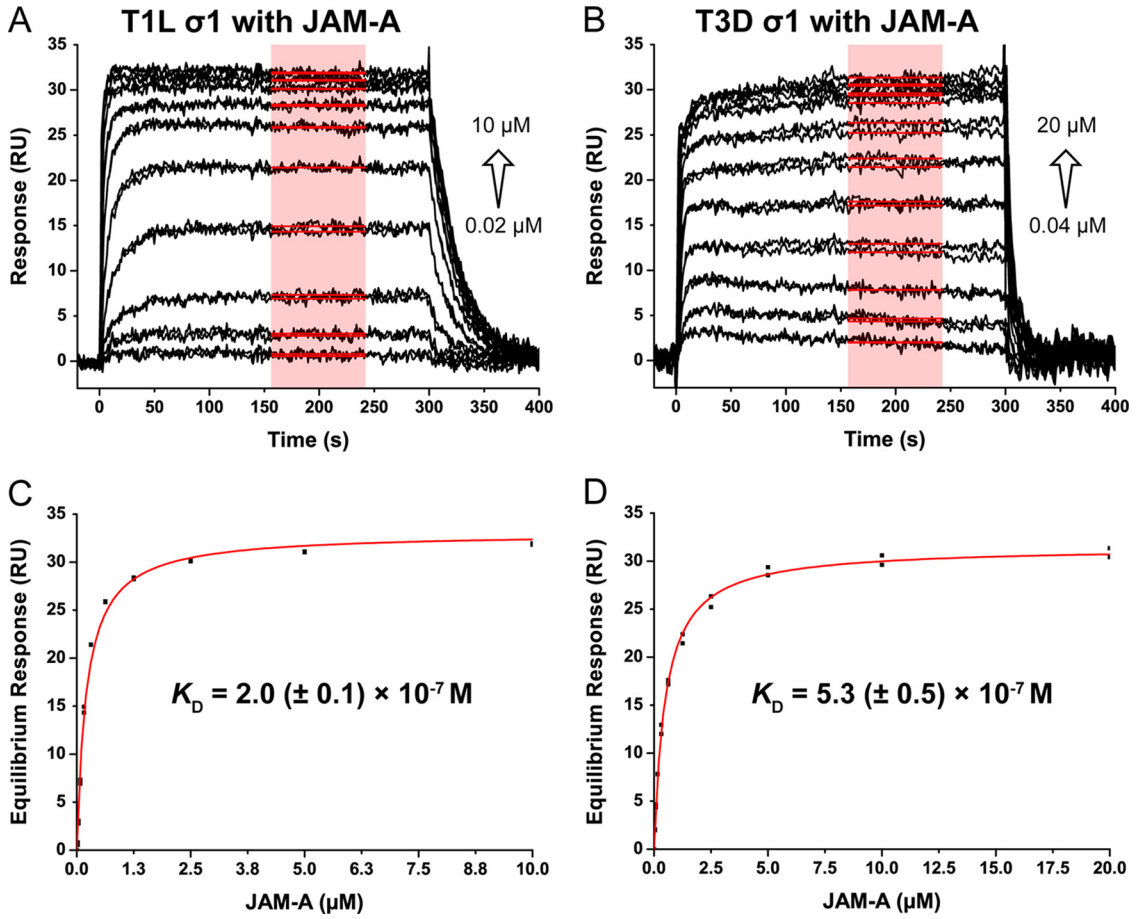

FIG 2 Representative SPR studies of JAM-A binding to σ1. Sensorgrams of 10 different concentrations of JAM-A (A, 0.02 to 10 μM; B, 0.04 to 20 μM) injected in duplicate over immobilized T1 σ1 (A) and T3 σ1 (B), respectively, at 25°C. Red boxes indicate the range used for calculation of equilibrium response values. (C and D) Curves of JAM-A binding to T1 σ1 (C) and T3 σ1 (D). The equilibrium response values are plotted against the injected JAM-A concentrations. The χ^2 values are 1.91 (C) and 0.27 (D); the R^2 values are 0.987 (C) and 0.998 (D). The average K_d values and standard deviations of several independent measurements are shown.

ceptors by σ1 influences serotype-dependent differences in tropism (20, 21). Differences in the tropism of T1 and T3 for ependymal cells and neurons, respectively, in the murine central nervous system segregate with the σ1-encoding S1 gene (22, 23). We currently are conducting experiments to define the domains in σ1 responsible for these tropism differences as part of another study. In this regard, the T1 and T3 σ1 proteins use different binding sites for sialylated glycan coreceptors (3, 6). T1 σ1 engages both JAM-A and the GM2 glycan with adjacent contact regions in the head domain, whereas the glycan binding site of T3 σ1 is located in the body domain. Despite the proximity of the two binding sites, both receptors can bind simultaneously to T1 σ1 (Fig. 3A) and also to T3 σ1 (6, 24). Comparison with the unliganded T1 σ1 head shows no significant structural changes upon JAM-A binding. Both structures superimpose with a root mean square deviation of 0.58 Å (Fig. 3B). Therefore, our data support a multistep adhesion-strengthening mechanism in which lower-affinity binding to carbohydrates guides the virus to target cells, while subsequent higher-affinity binding to JAM-A leads to stable attachment and primes the virus for entry (4).

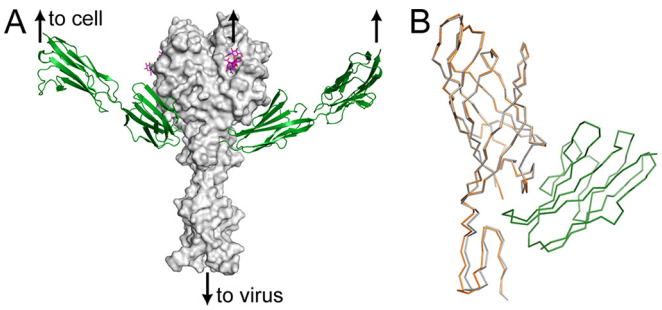

FIG 3 (A) Model of T1 σ1 bound to its two receptors. The σ1 protein (head domain and three β-spiral repeats) is shown in a surface representation (gray) in complex with GM2 shown in a stick representation (4GU3) (magenta) and JAM-A D1D2 (1NBQ) shown as a ribbon tracing (green). (B) Comparison of T1 σ1 in complex with JAM-A D1 and unliganded T1 σ1. A Cα tracing of the T1 σ1–JAM-A complex is shown with T1 σ1 in orange and JAM-A in green. One monomer of unliganded T1 σ1 is gray. Secondary-structure matching superpositions were calculated with Coot and CCP4 (16, 26, 27).

Protein structure accession numbers. Protein structural data have been deposited at the Protein Data Bank (PDB) under accession numbers 4ODB (T1 σ1–JAM-A complex) and 4XC5 (T1 σ1).

ACKNOWLEDGMENTS

We thank Kristen M. Ogden for careful review of the manuscript and the staff at the Swiss Light Source for beam time and technical support.

This work was supported by United States Public Health Service award R01 AI076983 and the Elizabeth B. Lamb Center for Pediatric Research. The funders had no role in study design, data collection and analysis, decision to publish, or preparation of the manuscript.

REFERENCES

1. **Barton ES, Forrest JC, Connolly JL, Chappell JD, Liu Y, Schnell FJ, Nusrat A, Parkos CA, Dermody TS.** 2001. Junction adhesion molecule is a receptor for reovirus. Cell **104:**441–451. http://dx.doi.org/10.1016/S0092-8674(01)00231-8.
2. **Campbell JA, Schelling P, Wetzel JD, Johnson EM, Forrest JC, Wilson GAR, Aurrand-Lions M, Imhof BA, Stehle T, Dermody TS.** 2005. Junctional adhesion molecule A serves as a receptor for prototype and field-isolate strains of mammalian reovirus. J Virol **79:**7967–7978. http://dx.doi.org/10.1128/JVI.79.13.7967-7978.2005.
3. **Reiss K, Stencel JE, Liu Y, Blaum BS, Reiter DM, Feizi T, Dermody TS, Stehle T.** 2012. The GM2 glycan serves as a functional coreceptor for serotype 1 reovirus. PLoS Pathog **8:**e1003078. http://dx.doi.org/10.1371/journal.ppat.1003078.
4. **Barton ES, Connolly JL, Forrest JC, Chappell JD, Dermody TS.** 2001. Utilization of sialic acid as a coreceptor enhances reovirus attachment by multistep adhesion strengthening. J Biol Chem **276:**2200–2211. http://dx.doi.org/10.1074/jbc.M004680200.
5. **Gentsch JR, Pacitti AF.** 1987. Differential interaction of reovirus type 3 with sialylated receptor components on animal cells. Virology **161:**245–248. http://dx.doi.org/10.1016/0042-6822(87)90192-9.
6. **Reiter DM, Frierson JM, Halvorson EE, Kobayashi T, Dermody TS, Stehle T.** 2011. Crystal structure of reovirus attachment protein σ1 in complex with sialylated oligosaccharides. PLoS Pathog **7:**e1002166. http://dx.doi.org/10.1371/journal.ppat.1002166.
7. **Paul RW, Choi AH, Lee PW.** 1989. The alpha-anomeric form of sialic acid is the minimal receptor determinant recognized by reovirus. Virology **172:**382–385. http://dx.doi.org/10.1016/0042-6822(89)90146-3.
8. **Kirchner E, Guglielmi KM, Strauss HM, Dermody TS, Stehle T.** 2008. Structure of reovirus sigma1 in complex with its receptor junctional adhesion molecule-A. PLoS Pathog **4:**e1000235. http://dx.doi.org/10.1371/journal.ppat.1000235.
9. **Chappell JD, Prota AE, Dermody TS, Stehle T.** 2002. Crystal structure of reovirus attachment protein sigma1 reveals evolutionary relationship to adenovirus fiber. EMBO J **21:**1–11. http://dx.doi.org/10.1093/emboj/21.1.1.
10. **Harbury PB, Zhang T, Kim PS, Alber T.** 1993. A switch between two-, three-, and four-stranded coiled coils in GCN4 leucine zipper mutants. Science **262:**1401–1407. http://dx.doi.org/10.1126/science.8248779.
11. **Harbury PB, Kim PS, Alber T.** 1994. Crystal structure of an isoleucine-zipper trimer. Nature **371:**80–83. http://dx.doi.org/10.1038/371080a0.
12. **Kabsch W.** 1993. Automatic processing of rotation diffraction data from crystals of initially unknown symmetry and cell constants. J Appl Crystallogr **26:**795–800. http://dx.doi.org/10.1107/S0021889893005588.
13. **McCoy AJ, Grosse-Kunstleve RW, Adams PD, Winn MD, Storoni LC, Read RJ.** 2007. Phaser crystallographic software. J Appl Crystallogr **40:**658–674. http://dx.doi.org/10.1107/S0021889807021206.
14. **Adams PD, Grosse-Kunstleve RW, Hung LW, Ioerger TR, McCoy AJ, Moriarty NW, Read RJ, Sacchettini JC, Sauter NK, Terwilliger TC.** 2002. PHENIX: building new software for automated crystallographic structure determination. Acta Crystallogr D **58:**1948–1954. http://dx.doi.org/10.1107/S0907444902016657.
15. **Bricogne G, Blanc E, Brandl M, Flensburg C, Keller P, Paciorek W, Roversi P, Sharff A, Smart OS, Vonrhein C, Womack TO.** 2014. BUSTER version 2.10.0. Global Phasing Ltd., Cambridge, United Kingdom.
16. **Emsley P, Lohkamp B, Scott WG, Cowtan K.** 2010. Features and development of Coot. Acta Crystallogr D **66:**486–501. http://dx.doi.org/10.1107/S0907444910007493.
17. **Schrödinger LLC.** 2010. The PyMOL molecular graphics system, version 1.5.0.5. Schrödinger LLC, New York, NY.
18. **Schelling P, Guglielmi KM, Kirchner E, Paetzold B, Dermody TS, Stehle T.** 2007. The reovirus sigma1 aspartic acid sandwich: a trimerization motif poised for conformational change. J Biol Chem **282:**11582–11589. http://dx.doi.org/10.1074/jbc.M610805200.
19. **Prota AE, Campbell JA, Schelling P, Forrest JC, Watson MJ, Peters TR, Aurrand-Lions M, Imhof BA, Dermody TS, Stehle T.** 2003. Crystal structure of human junctional adhesion molecule 1: implications for reovirus binding. Proc Natl Acad Sci U S A **100:**5366–5371. http://dx.doi.org/10.1073/pnas.0937718100.
20. **Frierson JM, Pruijssers AJ, Konopka JL, Reiter DM, Abel TW, Stehle T, Dermody TS.** 2012. Utilization of sialylated glycans as coreceptors enhances the neurovirulence of serotype 3 reovirus. J Virol **86:**13164–13173. http://dx.doi.org/10.1128/JVI.01822-12.
21. **Stencel-Baerenwald JE, Reiss K, Blaum BS, Colvin D, Li X-N, Abel TW, Boyd KL, Stehle T, Dermody TS.** 2015. Glycan engagement dictates hydrocephalus induction by serotype 1 reovirus. mBio **6:**e02356-14. http://dx.doi.org/10.1128/mBio.02356-14.
22. **Weiner HL, Drayna D, Averill DR, Fields BN.** 1977. Molecular basis of reovirus virulence: role of the S1 gene. Proc Natl Acad Sci U S A **74:**5744–5748. http://dx.doi.org/10.1073/pnas.74.12.5744.
23. **Weiner HL, Powers ML, Fields BN.** 1980. Absolute linkage of virulence and central nervous system cell tropism of reoviruses to viral hemagglutinin. J Infect Dis **141:**609–616. http://dx.doi.org/10.1093/infdis/141.5.609.
24. **Chappell JD, Duong JL, Wright BW, Dermody TS.** 2000. Identification of carbohydrate-binding domains in the attachment proteins of type 1 and type 3 reoviruses. J Virol **74:**8472–8479. http://dx.doi.org/10.1128/JVI.74.18.8472-8479.2000.
25. **Larkin MA, Blackshields G, Brown NP, Chenna R, McGettigan PA, McWilliam H, Valentin F, Wallace IM, Wilm A, Lopez R, Thompson JD, Gibson TJ, Higgins DG.** 2007. Clustal W and Clustal X version 2.0. Bioinformatics **23:**2947–2948. http://dx.doi.org/10.1093/bioinformatics/btm404.
26. **Winn MD, Ballard CC, Cowtan KD, Dodson EJ, Emsley P, Evans PR, Keegan RM, Krissinel EB, Leslie AGW, McCoy A, McNicholas SJ, Murshudov GN, Pannu NS, Potterton EA, Powell HR, Read RJ, Vagin A, Wilson KS.** 2011. Overview of the CCP4 suite and current developments. Acta Crystallogr D **67:**235–242. http://dx.doi.org/10.1107/S0907444910045749.
27. **Krissinel E, Henrick K.** 2004. Secondary-structure matching (SSM), a new tool for fast protein structure alignment in three dimensions. Acta Crystallogr D **60:**2256–2268. http://dx.doi.org/10.1107/S0907444904026460.
28. **Diederichs K, Karplus PA.** 1997. Improved R-factors for diffraction data analysis in macromolecular crystallography. Nat Struct Biol **4:**269–275. http://dx.doi.org/10.1038/nsb0497-269.
29. **Brünger AT.** 1992. Free R value: a novel statistical quantity for assessing the accuracy of crystal structures. Nature **355:**472–475. http://dx.doi.org/10.1038/355472a0.
30. **Lovell SC, Davis IW, Arendall WB, de Bakker PIW, Word JM, Prisant MG, Richardson JS, Richardson DC.** 2003. Structure validation by Calpha geometry: phi,psi and Cbeta deviation. Proteins **50:**437–450. http://dx.doi.org/10.1002/prot.10286.